

Optical and Shielding Parameters of Tellurite Glass with Composition 80TeO_2 - $5\text{Nb}_2\text{O}_5$ - 10ZnO - 5LiF for Medical Application: Theoretical Investigation

Khalid I Hussein^{1,2*}

¹Department of Radiological Sciences, College of Applied Medical Sciences, King Khalid University, Abha, Saudi Arabia

²Department of Medical Physics and Instrumentation, National Cancer Institute, University of Gezira, Wad Medani, Sudan

Abstract

The use of heavy metal oxide as shielding material attracted great interest among researchers in recent years due to its high shielding efficiency without loss of transparency, good physical properties, good thermal stability, and good optical properties. In this work, the physical, optical, and shielding effectiveness of tellurite glass with composition “ 80TeO_2 - $5\text{Nb}_2\text{O}_5$ - 10ZnO - 5LiF ” (TNZL) were investigated at photon energies range between 15 keV and 15 MeV. The shielding parameters of the proposed glass system such as linear attenuation coefficients, half value layer (HVL), the mean free path (MFP), effective atomic number (Z_{eff}), effective electron number (N_{eff}), and the optical properties such as the oxygen packing density (OPD), the molar refraction (R_m), and the molar electronic polarizability (α_m) were investigated. The present glass showed a superior performance at the diagnostic energy range between 40 keV and 80 keV. The maximum values of the percentage differences between the prepared sample and the standard materials were recorded at 40 keV. The maximum value of Z_{eff} (49.7) was recorded at 40 keV, while the minimum value (21.8) was recorded at 1.5 MeV.

Keywords

Tellurite glasses, Optical parameters mass attenuation coefficient, Linear attenuation coefficient, Half-value layer, Mean free path

Introduction

The use of ionizing radiation in the medical field increases dramatically over the past few years due to the increasing use of computed tomography examination in addition to the medical application of radiation in cancer treatment [1-3]. The severity of radiation injuries depends on the radiation exposure dose rate. The radiation risk and injuries

in the different applications were widely addressed by several researchers [4-8].

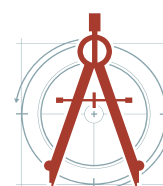
The use of ionizing radiation required safety standards to be established and implement to ensure the protection of people and the environment, many standards for radiation protection and safety were established [9-12]. Exposure time, distance from the source, and shielding are the basic prin-

***Corresponding author:** Khalid I Hussein, Department of Radiological Sciences, College of Applied Medical Sciences, King Khalid University, Abha 61421, Saudi Arabia

Accepted: August 03, 2021; **Published:** August 05, 2021

Copyright: © 2021 Hussein KI. This is an open-access article distributed under the terms of the Creative Commons Attribution License, which permits unrestricted use, distribution, and reproduction in any medium, provided the original author and source are credited.

Hussein. Int J Opt Photonic Eng 2021, 6:036



Citation: Hussein KI (2021) Optical and Shielding Parameters of Tellurite Glass with Composition 80TeO_2 - $5\text{Nb}_2\text{O}_5$ - 10ZnO - 5LiF for Medical Application: Theoretical Investigation. Int J Opt Photonic Eng 6:036

ciples of protection considered when dealing with ionizing radiation. Shielding is the most important consideration for any facility that performs diagnostic or therapy procedures. Many factors affecting the effectiveness of a shielding material used to protect people working in radiation facilities such as radiation energy, radiation type, the thickness of shielding material. The denser the material the more effective shielding materials against X-rays and gamma rays. Lead is the most common material use in most radiation applications as shielding material due to its high atomic number. Although, lead is the most effective material in attenuating gamma and X-ray photons but can cause pollution through the release of lead particles and can affect all the system body [13-15].

Several studies have been conducted to develop alternative materials that replace lead such as tellurite base glasses, phosphate-based materials, metal alloy, polymers [16-25]. These studies showed a good shielding performance in terms of high shielding efficiency without loss of transparency, good physical properties, thermal stability, and good optical properties.

The shielding effectiveness has been studied in terms of the physical properties, radiation shielding parameters, LAC, MAC, HVL, MFP, Z_{eff} , and N_{eff} . Hussein, et al. [16] have studied the shielding effectiveness of four novel tellurite-based glasses samples doped with oxide metals (75TeO₂-10P₂O₅-10ZnO-5PbF₂-0.24Er₂O₃; 70TeO₂-10P₂O₅-10ZnO-5PbF₂-5MgO-0.24Er₂O₃; 70TeO₂-10P₂O₅-10ZnO-5PbF₂-5BaO-0.24Er₂O₃; and 70TeO₂-10P₂O₅-10ZnO-5PbF₂-5SrO. Their results showed the prepared sample that contains Barium Oxide (BaO) has superior shielding effectiveness compared with other samples. Sayyed, et al. [20] have studied the performance of tellurite glasses system with different oxides at photon energy ranging between 1 keV to 100 GeV. The results showed that the two systems (TeO₂-WO₃ and TeO₂-B₂O₃) have superior shielding properties for gamma-ray and neutrons, respectively. Al-Hadeethi, et al. [21] have studied the X-ray photons attenuation characteristics for

two glass-based systems (Bi₂O₃-B₂O₃-TeO₂-TiO₃ and PbO-ZnO-TeO₂-B₂O₃) at photon energies ranging from 30 to 80 kVp. Their results showed that the increase of Tellurium dioxide (TeO₂) concentration increases the attenuation coefficients of the glass system with a decrease in the half-value layer especially at photon energy range between 70 and 80 keV. Lakshminarayana, et al. [22] have studied the radiation shielding effectiveness of borosilicate glasses doped Tm³⁺ ions for gamma application. Their results indicate that the sample that contains the highest mole concentration of Tm₂O₃ has the greater ability to attenuate gamma-rays.

In this work, the shielding effectiveness of Tellurite based-glass system was investigated at the photon energy range between 15 keV and 15 MeV. The radiation shielding parameters and the optical parameters of the prepared glass system such as LAC, MAC, HVL, Z_{eff} , Z_{eq} , MFP, N_{eff} were calculated using the online developed software (Phy-X/PSD) [24]. The optical properties of the prepared glass were also investigated. Computed values were compared with other commercial shielding materials commonly used in photon applications.

Theory and Method

A Tellurite glass sample contains different oxides (80TeO₂-5Nb₂O₅-10ZnO-5LiF) was prepared by putting the raw material in the platinum crucible in the heating furnace at a temperature in the range from 850 to 950 °C for 30 min. The melting material was stirred to increase the viscosity before cast in the brass mold. The prepared sample was put in the annealing furnace for 2 h at 320 °C. The sample density was measured using Archimedes' Principle. Table 1 shows the density, molar weight (M_w), and chemical compositions of the prepared sample.

The average molar weight of mixtures \bar{M} can be calculated using mole by fractions x_i and molar masses M_i of the constituent elements of the component using the following equation [25]:

$$\bar{M} = \sum x_i M_i \quad (1)$$

Where x_i is the molar fraction of each

Table 1: The Physical parameters and chemical compositions of the proposed glass samples.

Sample code	Mw (g/mol)	Density (g/cm ³) ± 0.04	Composition (mol%)			
			TeO ₂	Nb ₂ O ₅	ZnO	LiF
TNZL	150.4	5.231	80	5	10	5

component i , M_i is the molecular weight of the sample.

The molar volume (V_M) of glass material can be calculated by the following equation [25]:

$$V_M = \frac{\bar{M}}{\rho}, \quad (2)$$

Where M is the average molar weight of the sample, ρ is the density of the sample.

$$OPD = 1000 \sum x_i n_i \left(\frac{1}{V_M} \right), \quad (3)$$

Where V_M is the molar volume of the glass materials, n_i is a molar fraction, n_i is the number of oxygen atoms in each oxide. The molar refraction of R_m can be calculated using the following equation [25]:

$$R_m = \frac{n^2 - 1}{n^2 + 2} \times V_m, \quad (4)$$

The reflection loss, R_L in percentage, can be calculated using the following equation [25]:

$$R_L = \left[\frac{(n-1)}{(n+1)} \right]^2, \quad (5)$$

Where n is the refractive index of the glass material. The molar electronic polarizability (α_m) can be calculated using the following equation [25]:

$$\alpha_m = \frac{R_m}{2.52}, \quad (6)$$

The effectiveness of a shielding material can be investigated by the physical properties and radiation shielding parameters. The MAC, LAC, Z_{eff} , N_{eff} , HVL and MFP are the most important radiation shielding parameters that characterizing the effectiveness of the shielding materials. Cross section for scattering and absorption can be express in term of the total mass attenuation coefficient (μ/ρ), which can be calculated using the program Xcom [26]. The mass attenuation coefficient of a compound can be computed using the following relation [26-30]:

$$\frac{\mu}{\rho} = \sum_i w_i \left(\frac{\mu}{\rho} \right)_i \quad (7)$$

Where w_i is the fraction by weight of the i^{th} atomic element and $\left(\frac{\mu}{\rho} \right)_i$ is the mass attenuation of the of the i^{th} atomic element.

The probability of photon interaction with material can be characterized by the total atom cross-section (σ_a) and total electronic cross-section (σ_e) using the following relations [29,30]:

$$\sigma_a = \frac{1}{N_A} \sum_i f_i A_i \left(\frac{\mu}{\rho} \right)_i \quad (8)$$

$$\sigma_e = \frac{1}{N_A} \sum_j f_j \frac{A_j}{Z_j} \left(\frac{\mu}{\rho} \right)_j \quad (9)$$

Where f_i is fraction by mole of the i^{th} atomic element, A_i is atomic weight of the i^{th} atomic element, Z_j is atomic number and N_A is Avogadro constant.

The effective atomic number which varies with energies can be calculated from the ratio of atomic and electronic cross-sections by the following relation [29,30]:

$$Z_{eff} = \frac{\sigma_a}{\sigma_e} \quad (10)$$

The effective electron number (N_{eff}) is representing the number of electrons per unit mass of the shielding material can be computed using the following relation [29,30]:

$$N_e = \frac{N_A}{A} Z_{eff} \quad (11)$$

Where A is the mean atomic mass equal to $\sum_i f_i A_i$; f_i is fraction by mole of the i^{th} atomic element, A_i is atomic weight of the i^{th} atomic element.

The half-value layer (HVL) and the mean free pass (MFP) are considered as important parameters for the estimation of the required effective shielding thickness for each photon energy. The HVL is the required thickness to reduce radiation intensity of the mono-energetic beam to its half value, while the MFP is representing the average distance between two successive interaction. These parameters can be computed according to the following relations [29,30]:

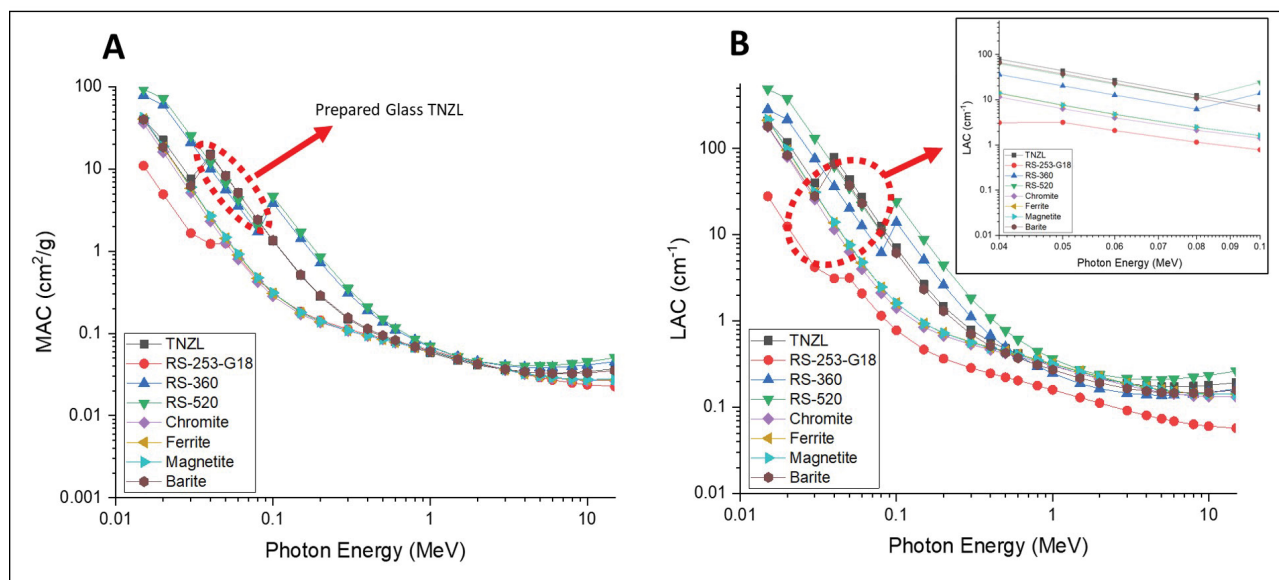
$$HVL = \frac{0.693}{\mu} \quad (12)$$

$$MFP = \frac{1}{\mu} \quad (13)$$

Where μ is the linear attenuation coefficient.

Table 2: The optical properties of the prepared sample compared with RS 253 G18, RS 520, and RS 360.

Sample code	Refractive Index @ $\lambda = 535$ nm	OPD (mol/l)	R _m (m ³)	α_m ($\times 10^{-24} \cdot \text{cm}^3$)
TNZL	2.14	67.82	15.61	6.19
RS 253 G18	1.52	71.18	8.2	3.25
RS 360	1.62	38.22	13.32	5.29
RS 520	1.81	37.45	14.62	5.80

**Figure 1:** The LAC (A), and MAC (B) values for prepared glass sample compared with some common commercial shielding materials at photon energy range between 15 Kev and 15 MeV.

Results and Discussion

Table 2 shows the optical properties of the prepared sample. The oxygen packing density (OPD), the molar refraction (R_m), and the molar electronic polarizability (α_m) of the prepared sample compared with some commercially available glass shielding materials such as that developed by Schott Co., Germany standard shielding glass materials (RS 253 G18, RS 520, and RS 360) [31]. The measured refractive index at wavelength 535 nm of the prepared sample recorded the highest value compared with the refractive indices of standard materials taken from the literature [31]. As shown in Table 2, the prepared sample recorded high values compared with other glass systems. This indicates that the proposed glass has more non-bridging oxygen, which improves the stability of glass as a host matrix for rare earth elements.

Figure 1A and Figure 1B show the computed linear and mass attenuation coefficients (LAC,

MAC) of the prepared sample compared with some commercially available shielding materials such as Schott Co., Germany standard shielding glass materials (RS 253 G18, RS 520, and RS 360) [31] and some common oxide used with concrete materials such as Chromite, Ferrite, Magnetite and Barite [32] at energy range between 15 keV and 15 MeV. The LAC and MAC for the prepared sample were computed using the online developed software (Phy-X/PSD) [24]. As shown in Figure 1A and Figure 1B, the prepared sample show superior performance in terms of shielding effectiveness in the diagnostic energy range between 40 keV and 80 keV compared with the standard materials. In addition to that, the prepared sample shows good performance in the higher photon energies (> 1 MeV). For example, the value of mass attenuation coefficient recorded of prepared sample was $12.5 \text{ cm}^2/\text{g}$ compared to 1.15, 6.19, 10.63, 2.11, 2.45, 2.47 and $10.86 \text{ cm}^2/\text{g}$ at 80 keV, with percentage differences of 90.8%, 50.6%, 15.2%, 83.2%, 80.5%,

80.3% and 13.5% for the RS 253 G18, RS 360, RS 520, Chromite, Chromite, Ferrite, Magnetite and Barite respectively. As shown in Figures 1A and Figure 1B the mass and the linear attenuation coefficients decrease as the photon energy increased. This is due to the contribution of the photoelectric effect, Compton scattering, and pair production which are the most predominant interactions in the diagnostic and therapeutic energies range.

Figure 2A and Figure 2B show the computed

half-value layers (HVL) and mean free path (MFP) of the prepared sample compared with some commercially available standard (RS 253 G18, RS 360, RS 520, Chromite, Chromite, Ferrite, Magnetite, and Barite) at energy range between 15 keV and 15 MeV. The HVL and MFP are mainly depending on the linear attenuation of glass samples. As shown in the Figure 2A and Figure 2B the recorded HVL and MFP values of prepared sample is lower than the values recorded for standard materials at energy range between 40 keV and 80 keV and at

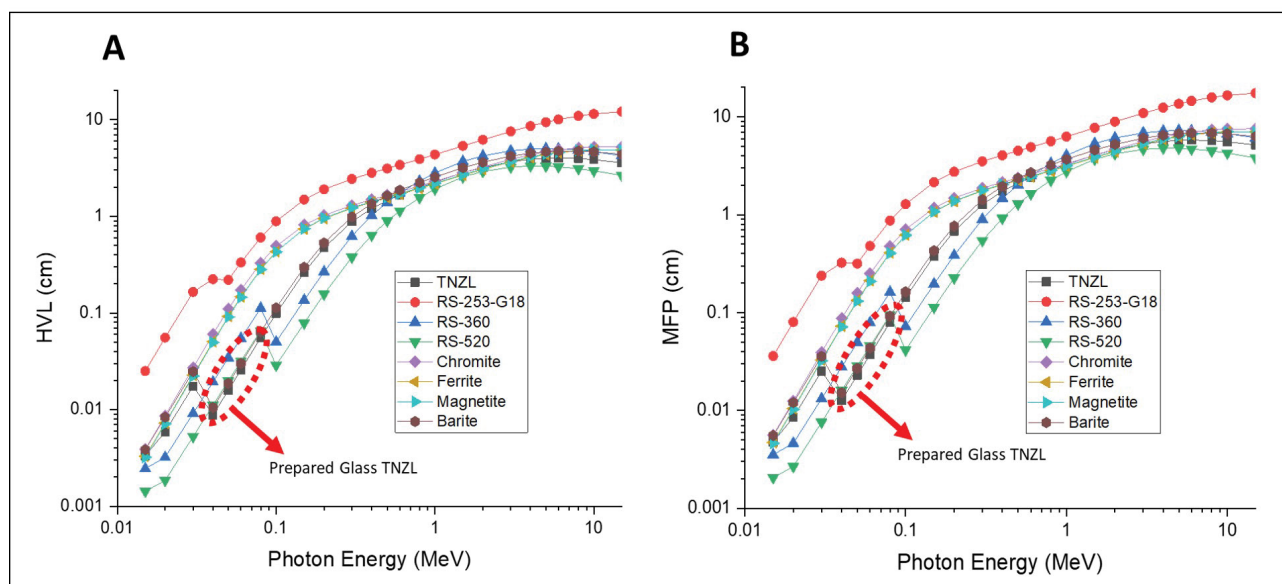


Figure 2: The HVL (A), and MFP (B) values for prepared glass sample compared with some common commercial shielding materials at photon energy range between 15 Kev and 15 MeV.

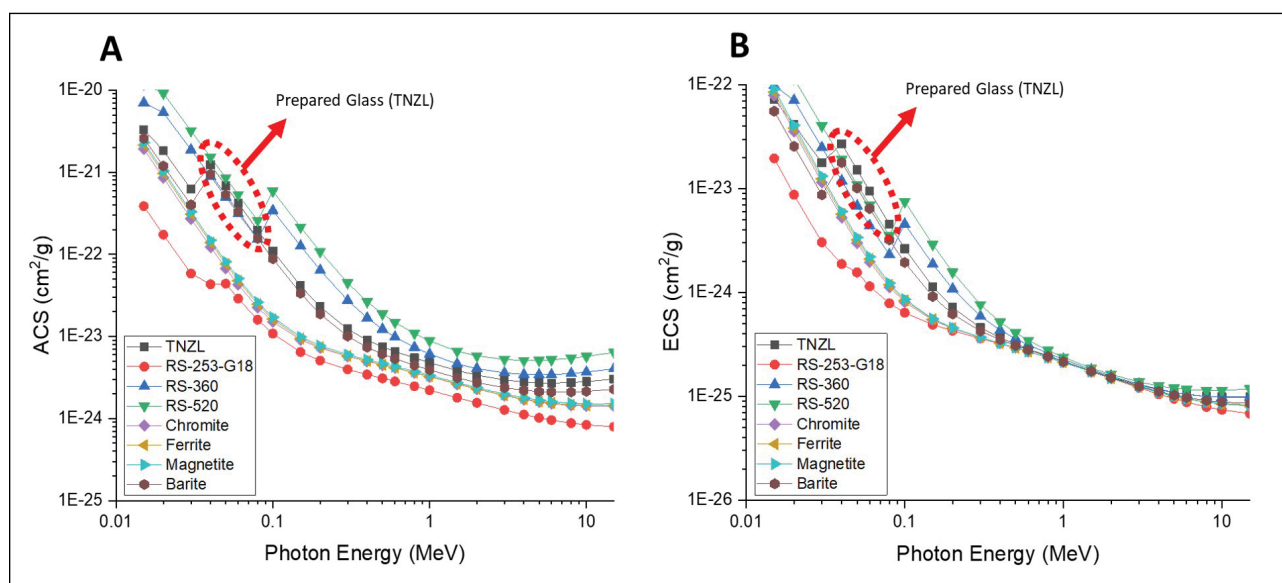


Figure 3: The ACS (A), and ECS (B) values for prepared glass sample compared with some common commercial shielding materials at photon energy range between 15 Kev and 15 MeV.

higher photon energies. These recoded values of HVL and MFP are expected due to the higher linear attenuation recorded for the sample compared with other samples. For example, the computed HVL value of the prepared sample was found 3.21 cm compared to 6.20, 4.22, 3.24, 3.10, 3.1, and 3.63 cm at 80 keV, with percentage differences of 93.00%, 31.50%, 1.05%, 4.75%, 3.44% and 13.08% for RS 253 G18, RS 360, Chromite, Chromite, Ferrite, Magnetite and Barite respectively. The prepared sample recorded slightly higher values than RS 520, which is expected due to a higher concentration of lead oxide in the RS 520 (71%) glass system.

Figure 3 shows the values of the total atom cross-section (ACS) and total electronic cross-section (ECS) as a function of photon energy for the prepared samples materials. The prepared sample recorded comparable values of ACS and ECS when compared with the common commercial shielding materials specifically in the diagnostic range between 40 and 80 keV as indicated in Figure 3. The recorded values of the prepared sample, which an indication of better efficiency of the sample as a shielding material compared with the other samples. These results consistent with findings discussed before for linear and mass attenuation.

Figure 4A and Figure 4B illustrated the effective atomic number (Z_{eff}) and effective electron numbers (N_{eff}) against photon energy (MeV) of the prepared glass samples. As shown in Figure 4A

the recorded values of effective atomic number (Z_{eff}) are higher than the values recorded for the standard materials (RS 253 G18, Chromite, Ferrite, Magnetite, and Barite), while the prepared sample recorded slightly lower values compared to the commercial standard glasses RS-520 and RS-360, this is due to the high concentration of lead oxide in these standard materials. The values of the effective atomic number are slightly decreased due to the influence of the photoelectric absorption in low energy range, then decrease dramatically in the region where the Compton scatter is predominant before it rises again in the high energy region due to the effect of pair production.

Conclusion

Shielding, physical and optical properties of tellurite glass at photon energies range 15 keV and 15 MeV have been studied. The shielding parameters of the proposed glass such as the oxygen packing density, the molar refraction, and the molar electronic polarizability, linear and mass attenuation coefficients, half value layer, the mean free path, effective atomic number, effective electron number were evaluated. The prepared glass sample recorded comparable values of shielding and optical properties compared with the common standard materials. The proposed sample showed a superior performance at the diagnostic energy range between 40 keV and 80 keV. The maximum values of the percentage differences

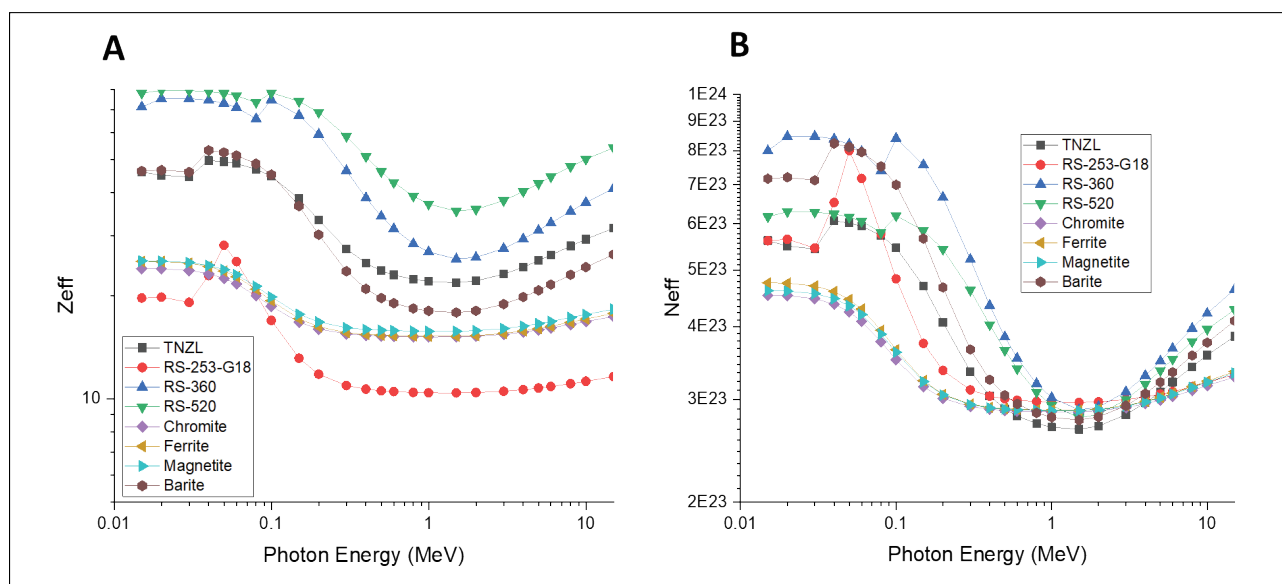


Figure 4: The Z_{eff} (A), and N_{eff} (B) values for prepared glass sample compared with some common commercial shielding materials at photon energy range between 15 Kev and 15 MeV.

between the prepared sample and the standard materials were recorded at 40 keV. The maximum value of Z_{eff} (49.7) was recorded at 40 keV, while the minimum value (21.8) was recorded at 1.5 MeV. These results show the efficacy of the prepared glass material as a promising shielding material in medical imaging as well as radiation therapy applications.

Acknowledgments

The authors extend their appreciation to the Deanship of Scientific Research at King Khalid University (KKU) - Saudi Arabia for funding this research project (Grant Code: R.G.P2/79/41).

References

- Parker HMOD, Joyce MJ (2015) The use of ionizing radiation to image nuclear fuel: A review. *Progress in Nuclear Energy* 85: 297-318.
- Vreysen MJB, Robinson AS (2011) Ionising radiation and area-wide management of insect pests to promote sustainable agriculture. *Sustainable Agriculture* 2: 671-692.
- Smith-Bindman R, Miglioretti DL, Larson EB (2008) Rising use of diagnostic medical imaging in a large integrated health system. *Health Aff (Millwood)* 27: 1491-1502.
- Meulepas JM, Ronckers CM, Smets AMJB, Nievelstein RAJ, Gradowska P, et al. (2018) Radiation exposure from pediatric CT scans and subsequent cancer risk in the Netherlands. *J Natl Cancer Inst* 111: 256-253.
- Mathews JD, Forsythe AV, Brady Z, Butler MW, Goergen SK, et al. (2013) Cancer risk in 680,000 people exposed to computed tomography scans in childhood or adolescence: Data linkage study of 11 million Australians. *BMJ* 346: 2360.
- Linnet MS, Slovis TL, Miller DL, Kleinerman R, Lee C, et al. (2012) Cancer risks associated with external radiation from diagnostic imaging procedures. *CA Cancer J Clin* 62: 75-100.
- Hall EJ, Brenner DJ (2012) Cancer risks from diagnostic radiology: The impact of new epidemiological data. *Br J Radiol* 85: e1316-e1317.
- Committee to assess health risks from exposure to low levels of ionizing radiation NRC (2006) Health risks from exposure to low levels of ionizing radiation: BEIR VII Phase 2. National Academies Press, Washington.
- https://www-pub.iaea.org/MTCD/Publications/PDF/PUB1775_web.pdf
- <https://www-pub.iaea.org/MTCD/publications/PDF/Pub1650web-23654722.pdf>
- (2007) The 2007 recommendations of the international commission on radiological protection. ICRP publication 103. *Ann ICRP* 37: 1-332.
- International Atomic Energy Agency (2007) IAEA safety glossary: Terminology used in nuclear safety and radiation protection (2007 Edition). IAEA, Vienna.
- Shoag JM, Burns KM, Kahlon SS, Parsons PJ, Bijur PE, et al. (2020) Lead poisoning risk assessment of radiology workers using lead shields. *Arch Environ Occup Health* 75: 60-64.
- Anink D, Boonstra C, Mak J (1996) Handbook of sustainable building. James & James, London.
- Balanli A, Ozturk A, Yapinli I (1995) Examining indoor and outdoor environments of buildings in terms of building biology. Healthy cities and civil engineering symposium, Chamber of Turkish Civil Engineers, Izmir Branch 45-55.
- Hussein KI, Alqahtani MS, Grelowska I, Reben M, Afifi H, et al. (2021) Optically transparent glass modified with metal oxides for X-rays and gamma rays shielding material. *J Xray Sci Technol* 29: 331-345.
- Alqahtani MS, Almarhaby AM, Hussein KI, AbouDeif YM, Afifi H, et al. (2021) Radiation attenuation and photoluminescence properties of host tellurite glasses doped with Er^{3+} . *Journal of Instrumentation* 16.
- Gedikoğlu N, Ersundu A, Aydin S, Çelikbilek M (2018) Crystallization behavior of WO_3 - MoO_3 - TeO_2 glasses. *J Non-Cryst Solids* 501: 93-100.
- Tekin HO, Kassab LRP, Kilicoglu O, Magalhães ES, Shams AM, et al. (2019) Newly developed tellurium oxide glasses for nuclear shielding applications: An extended investigation. *J Non-Cryst Solids* 528: 119763.
- Sayyed MI (2016) Investigations of gamma ray and fast neutron shielding properties of tellurite glasses with different oxide compositions. *Canadian Journal of Physics* 94.
- Al-Hadeethi Y, Sayyed MI, Mohammed H, Rimondin L (2020) X-ray photons attenuation characteristics for two tellurite-based glass systems at dental diagnostic energies. *Ceram Int* 46: 251-257.
- Lakshminarayana G, Sayyed MI, Baki SO, Lira A, Dong M, et al. (2018) Absorption and gamma-radiation-shielding parameter studies of Tm^{3+} -doped multicomponent borosilicate glasses. *Applied Physics A* 124: 1-16.

23. Mhareb M, Almessiere M, Sayyed MI, Alajerami Y (2019) Physical, structural, optical and photons attenuation attributes of lithium-magnesium-borate glasses: Role of Tm_2O_3 doping. *Optik* 182: 821-831.
24. Şakar E, Özpolat ÖF, Alım B, Sayyed MI, Kurudirek M (2020) Phy-X/PSD: Development of a user-friendly online software for calculation of parameters relevant to radiation shielding and dosimetry. *Radiation Physics and Chemistry* 166: 108496.
25. Kıbrıslı O, Ersundu AE, Çelikkilek EM (2019) Dy^{3+} doped tellurite glasses for solid-state lighting: An investigation through physical, thermal, structural and optical spectroscopy studies. *Journal of Non-Crystalline Solids* 513: 125-136.
26. Hubbell JH, Seltzer SM (1995) Tables of X-Ray mass attenuation coefficients and mass energy-absorption coefficients 1 keV to 20 MeV for elements $Z=1$ to 92 and 48 additional substances of dosimetric interest. National Institute of Standards and Technology, Gaithersburg, USA.
27. Hubbell JH (1999) Review of photon interaction cross section data in the medical and biological context. *Phys Med Biol* 44: R1-R22.
28. Gerward L, Guilbert N, Jensen KB, Leving H (2004) WinXCom - a program for calculating X-ray attenuation coefficients. *Radiat Phys Chem* 71: 653-654.
29. Taylor ML, Smith RL, Dossing F, Franich RD (2012) Robust calculation of effective atomic numbers: The Auto-Z(eff) software. *Med Phys* 39: 1769-1778.
30. Un AD, Caner T (2014) The Direct-Z(eff) software for direct calculation of mass attenuation coefficient, effective atomic number and effective electron number. *Ann Nucl Energy* 65: 158-165.
31. <https://www.schott.com/en-us/products/radiation-shielding-glasses>
32. Kaundal RS (2016) Comparative study of radiation shielding parameters for bismuth borate glasses. *Materials Research* 19: 776-778.

